FINAL TECHNICAL REPORT FOR DE-FG02-04ER41317

Advanced Computation and Chaotic Dynamics for Beams and Accelerators

Applicant/Institution:	The Regents of the University of Colorado, Office of Contracts and Grants
Street Address/City/State/Zip:	3100 Marine Street, UCB 572, Boulder, CO 80309-0572
Principal Investigator:	John R. Cary
Address:	Department of Physics, University of Colorado, Boulder, CO 80309-390
Telephone Number:	303-492-1489
Email:	cary@colorado.edu
Administrative Point of Contact:	Victoria Johnston Victoria.Johnston@colorado.edu, 303-492-8760
DOE/Office of Science Program Office:	Office of High Energy Physics
DOE/Office of Science Program Manager Contact:	John Boger

September, 2014

Table of Contents

1. **OVERVIEW** 1
2. **WAKEFIELDS CODE COMPARISON FOR CLIC STRUCTURES** 1
3. **CHARACTERIZATION OF FABRICATED PHC FIBERS FOR ALL-DIELECTRIC, LASER-DRIVEN PHC ACCELERATOR STRUCTURES** 2
4. **INPUT POWER COUPLING FOR THE LIN FIBER** 3
5. **COMPUTATIONAL EM WITH ANISOTROPIC DIELECTRICS** 5
6. **EM ALGORITHMS WITH CURVED METAL BOUNDARIES: ACCURACY STUDY** 5
7. **IMPLICIT EM ALGORITHMS** 5
8. **RECENT PUBLICATIONS** 6

APPENDIX A: BIBLIOGRAPHY AND REFERENCES CITED 7

1. Overview

During the year ending in August 2013, we continued to investigate the potential of photonic crystal (PhC) materials for acceleration purposes. We worked to characterize acceleration ability of simple PhC accelerator structures, as well as to characterize PhC materials to determine whether current fabrication techniques can meet the needs of future accelerating structures. We have also continued to design and optimize PhC accelerator structures, with the ultimate goal of finding a new kind of accelerator structure that could offer significant advantages over current RF acceleration technology. This design and optimization of these requires high performance computation, and we continue to work on methods to make such computation faster and more efficient.

Earlier work led us to an optimized dielectric structure, based originally on a PhC cavity, but optimized far away from lattice symmetry. We subsequently calculated wakefields in PhC and optimized structures and compared them to state-of-the-art metal (CLIC) cavities. This year we checked our results by performing a code-comparison, working with colleagues at CERN to compare calculations of CLIC wakefields with two different codes.

We continued collaboration with colleagues SLAC who (in collaboraion with Incom) have been working to fabricate PhC fibers and test their properties using Fourier Transform Infrared Spectroscopy (FTIR); since it's far from obvious how FTIR results should be correlated with PhC properties, our effort focused on simulated the reflection/scattering of incoming monochromatic radiation on PhC fibers.

While PhC fibers are attractive because the fabrication of optical fibers has the potential to be easy and cheap, such fabrication does not include the difficulty of coupling power into an accelerating fiber structure. The difficulty is both theoretical and practical: theoretical because the incomplete bandgap of PhC fibers makes it more difficult to channel energy as desired, and practical because coupling designs tend to spoil the 2D nature (uniform in the third dimension) of fibers, which is the property that makes them relatively easy to fabricate. We have proposed a novel coupling method that could solve both these problems. First, we fix the wave-number in the axial direction, allowing us to work within the existing partial bandgap. Second, we have worked on a coupling design that is still uniform in the third dimension--at least for relatively long sections. We feel that this approach is the most promising approach so far investigated for coupling to PhC accelerating fibers.

To facilitate the computer-intensive simulation of electomagnetic waves in dielectric and metal structures, we developed algorithms for electromagnetics with an emphasis on embedded boundaries for curved material surfaces. In particular, we developed a more accurate algorithm for dielectric boundaries (that is also more stable for very high dielectric contrast), in the process gaining a greater understanding of the accuracy of previously-proposed dielectric algorithms. We also developed a truly second-order frequency-domain algorithm for curved metal boundaries and showed good parallel performance using the Trilinos matrix library.

On another front, we investigated implicit electromagnetic algorithms with the potential to allow more efficient simulations of cases with geometric features much smaller than the (free-space) wavelength. The alternating-direction-implicit method is an often-touted parallelizable algorithm allowing arbitrarily large time steps, even when spatial cell size is very small (compared to the product of the speed of light and the time step). We showed that parallel implementation is feasible, but tricky due to the need for global communication. However, a more in depth investigation revealed that the ADI algorithm--in its simplest form--is actually unsuitable for most of the problems for which it was designed. Nevertheless, there are corrections that might lead to suitable algorithms with a similar parallelization as the basic ADI method.

2. Wakefields code comparison for CLIC structures

A photonic crystal (PhC), a regular lattice of metal or dielectric objects, can reflect electromagnetic waves in (only) a narrow frequency range, while other frequencies propagate through. A cavity in a PhC can therefore trap just a single mode (or a few modes), potentially offering many benefits. In 2008, we optimized the positions of dielectric rods in a 2D PhC (Fig. 1)—away from the lattice configuration—to reduce the losses (or increase Q) by two orders of magnitude [1].

We returned to the study of aperiodic photonic cavities expected to reduce wakefields [2] compared to closed metal pillbox cavities. Full 3D simulations (with beam tubes) showed that periodic PhC structures have higher-than-expected wakefields [3,4], due to zero-group-velocity PhC modes, which necessarily exist at the band gap edges; moreover, they are likely to couple to a cavity mode in a typical PhC defect cavity. This explanation indicates that this result is generic, likely to be true for all structures achieving confinement through presence of a band gap.

On the other hand, the optimized (aperiodic) structure (Fig. 1) has much lower wakefields, comparable to the state-of-the-art CLIC design even though this structure was optimized to increase confinement of the accelerating mode (not specifically to reduce wakefields). This supports our explanation: the optimized configuration has no lattice periodicity, hence no band structure; therefore, it does not necessarily have zero-group-velocity modes.

To continue the comparison we worked with Hao Zha and Alexei Grudiev at CERN to verify our wakefield computations in CLIC structures. Fig. 2 (courtesy of Hao Zha) shows a wakefield comparison between Vorpal and Gdfidl for a fully-dressed CLIC accelerator cavity. The agreement was very good, except for the very long-term wakes, which were degraded in Vorpal due to a problem with reflections from the ends of the HOM-damping waveguides--a problem that was discussed in detail in Carl Bauer's thesis (and which didn't apply to our dielectric structures, but only to absorption at the end of metal waveguides).

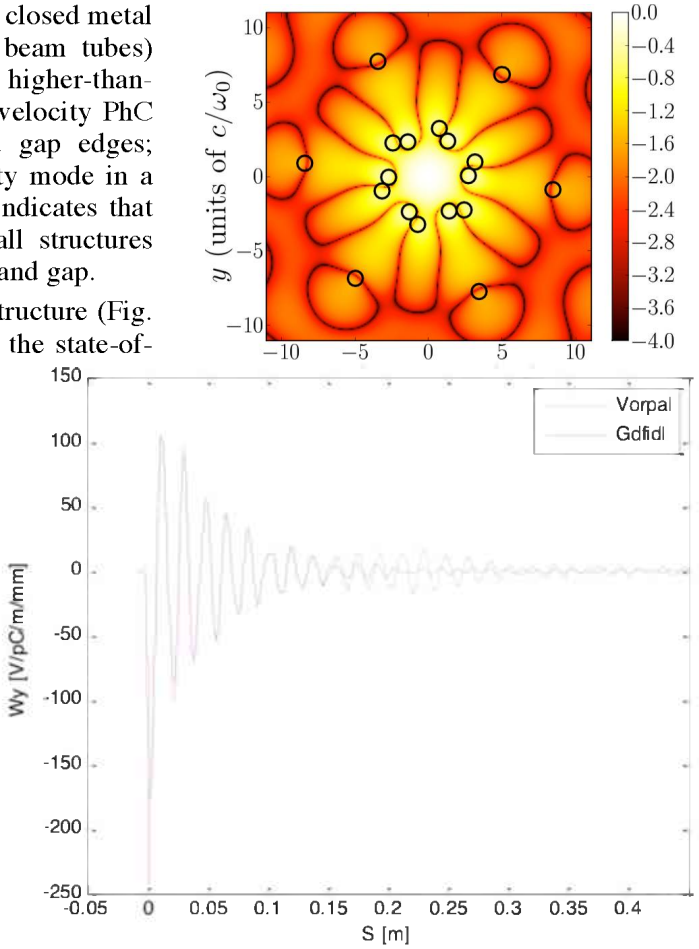

Fig. 2 Vorpal and Gdfidl wakefield calculations (credit: Hao Zha)

3. Characterization of fabricated PhC fibers for all-dielectric, laser-driven PhC accelerator structures

Acceleration with optical-frequency (i.e., laser-driven) electromagnetic fields would open up an entirely new regime for accelerators, hopefully allowing greater acceleration in shorter distances. In collaboration with the SLAC DLA group, we have been studying the properties of two very different designs: one based on optical fibers arranged in a 2D photonic crystal (PhC) [5], and the other based on the woodpile PhC [6]. Both these designs are of particular interest because prototypes are being fabricated at SLAC. We have tried to compute measurable properties of structures that will actually be tested—both to verify our computational algorithms, and to optimize the structure design. Figure 3 shows some transmission spectra for the PhC fiber, demonstrating one of our results: that oblique incidence from the fiber side is a much more sensitive probe of the lattice structure than end-on incidence (however, the former is a more difficult experiment to perform).

Matching the experimental Fourier Transform Infrared Spectroscopy (FTIR) results for end-on transmission (i.e., parallel to the fiber) has not been successful. We believe this is because transmission parallel to the fiber does not directly probe photonic crystal properties (the crystal structure of a fiber exists only in the 2D plane perpendicular to the fiber). Instead of measuring transmission and reflection due to band gaps, one measures transmission through a material with many transmission channels. Instead of distinct band gaps caused by dielectric contrast, one sees the effects of material absorption, and scattering by material defects. Our simulations did not take material absorption into account; moreover, the actual samples were thousands of wavelengths long, and our simulations could did not simulate such long distances. Although it would be interesting to try to simulate material absorption, it would also be very difficult, since such absorption is known to be very sensitive to the material history (such as the process by which the fiber was formed).

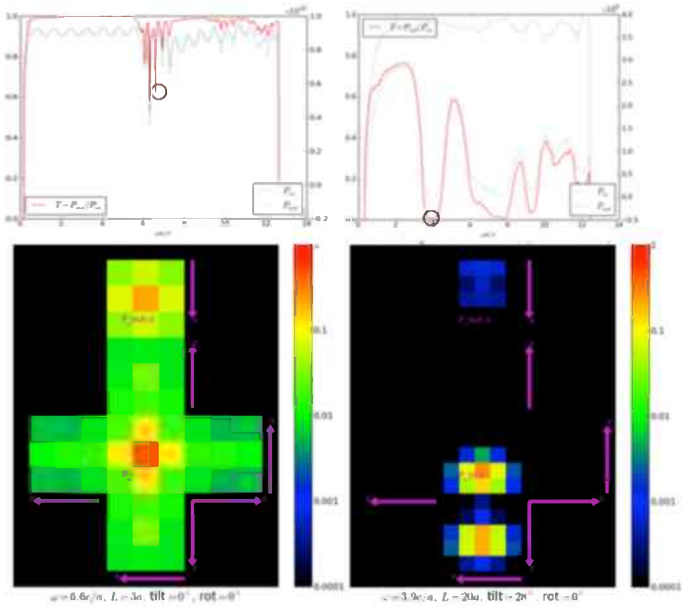

Fig. 3 Transmission vs. normalized frequency through a PhC fiber, with end-on incidence (top left) and side-illumination (top right), with power through simulation box walls (bottom).

In contrast, the oblique incidence experiments that we propose (but which are harder to perform) do probe the photonic crystal nature of the fiber. In contrast to end-on incidence (Fig. 3, upper left), just 10 or so wavelengths of fiber create dramatic drops in transmission with oblique incidence (Fig. 3, upper right). Furthermore, when we look at where light is scattered, end-on illumination results in significant transmission as well as somewhat uniform scattering out the sides (Fig. 3, lower left); there seem to be no special characteristics of the scattering (due the band structure). Oblique incidence, on the other hand, not only reduces transmission nearly to zero, but shows a completely different behavior: most light is back-scattered or reflected nearly specularly off the initial vacuum/glass interface. The specular reflection is not of much interest; it occurs in the oblique case simply because grazing incidence at a single dielectric transition causes more reflection that normal incidence. However, it is remarkable that, aside from the specular reflection, most light is backscattered, with a very small amount transmitted (so small, that it's possible this is actually going around the fiber and not through it), and even smaller amount side-scattered. This shows the effect of a band gap: light cannot propagate through the crystal (at frequencies within the band gap), so it is backscattered.

4. Input power coupling for the Lin fiber

Coupling into a photonic crystal fiber, such as the Lin fiber [5], is difficult because of the open nature of the PhC fiber and its lack of a complete 3D band gap: the 2D crystal structure creates only a 2D, hence partial, band gap. We have investigated a novel idea for taking advantage of the partial band gap of the PhC fiber, to couple power between adjacent "defect" channels in the fiber, such as might lead to the coupling scheme shown in Fig. 4.

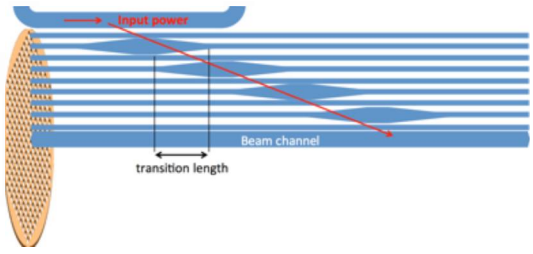

Fig. 4 Cascade coupling scheme for a fiber accelerator that preserves k_z.

The partial bandgap of a PhC fiber prevents any propagation of light within a small range of frequencies

and k_z (the axial wave number). To use the bandgap to trap fields capable of accelerating particles, the bandgap must be around $\omega/k_z=v$ (the beam velocity, essentially c for electrons/positrons). To take advantage of the band gap, we must work in this regime. For example, by coupling over a sufficient length, we can fix k_z and thereby stay within the band gap, preventing scattering to other modes.

The defect in the fiber (i.e., the enlarged central hole) allows propagation of a synchronous mode (which would otherwise be forbidden in the PhC due to the bandgap); unfortunately, more than one defect mode may be allowed.

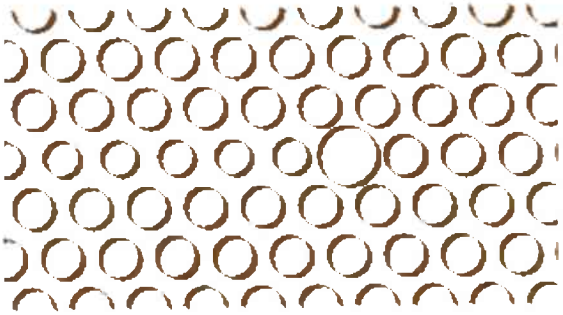

Fig. 5 A line of defects leading to the central defect.

We demonstrated proof-of-concept, by coupling from one defect channel to an adjacent channel (the beam channel). We successfully avoided coupling to bulk PhC modes (thanks to the band gap), but coupling to other defect modes is a problem. Symmetric coupling avoids transferring power to dipole modes, significantly increasing efficiency. For this initial geometry, we found that coupling efficiency (into the accelerating mode) rises to a maximum around 50% for a transition length around 30 lattice constants. Later we were able to increase coupling efficiency to 60% by adjusting the frequency slightly. While higher efficiency is still desired, this shows that the method is basically feasible--moreover, it shows that we are not only coupling power into the accelerating channel, but also that we are coupling power into the accelerating mode, something that has been a major challenge for other coupling schemes (which often have trouble exceeding 10% efficiency into the desired mode).

The ideal situation for acceleration--and, for that matter, for coupling--would be to have a defect channel that carries only a single mode, which is suitable for acceleration. This would avoid the problem of coupling into other defect modes, while the band gap would disallow coupling into any bulk PhC modes, thus completely trapping the fields in the desired accelerating mode. However, this situation is extremely hard to realize. Therefore, we expect the "cascade of defect channels" (Fig. 4) may present some difficulties. While we were able to avoid coupling into most defect modes using symmetric coupling (with 2 coupling channels on either side of the accelerating channel), future research would be needed to determine how each stage of the cascade could take advantage of this.

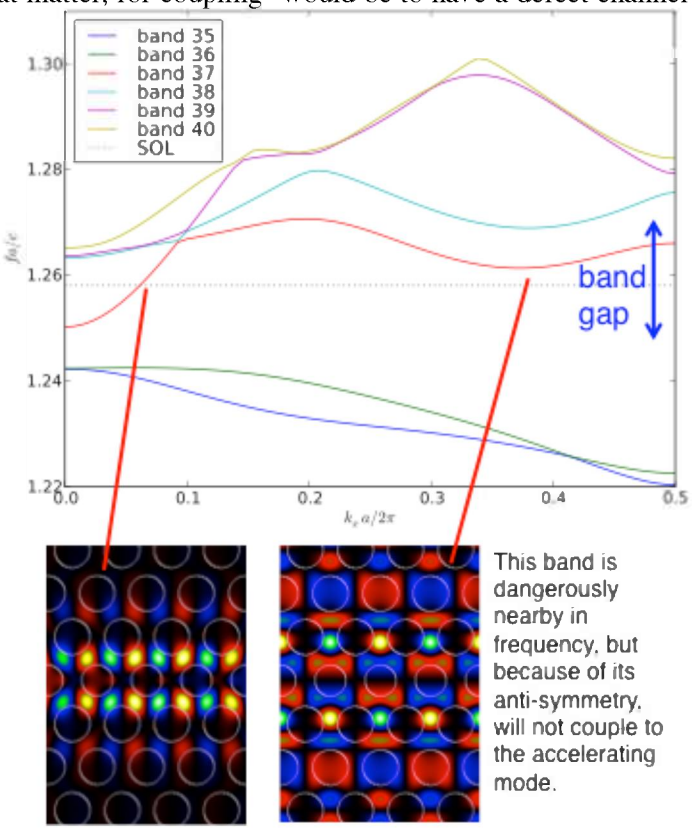

Fig. 6 Band diagram (top) showing line-defect coupling mode (crossing dotted line, field pattern at lower left) and other defect mode (lower right) with wrong symmetry.

We therefore began to investigate an approach that incorporates perpendicular propagation (from the outside to the inside of the fiber). Again, working in the regime of fixed k_z, we consider a "line defect" from the outside to the inside of the crystal (Fig. 5; the holes in a line left of the central defect are smaller than the rest). The line defect acts like a waveguide for fixed k_z, allowing us to propagate a mode from the outside to the inside of the fiber. Moreover, this line defect is uniform in the z-direction, which would make it much easier to fabricate than the

cascade of Fig. 4.

Ideally, the line defect mode would be isolated, with no other defect modes at nearby frequency or k_z. Although scattering into other defect modes is not a problem once the defect mode is excited, exciting the defect mode in the first place (on the outside of the fiber) will be easier if the defect mode is isolated. In this case, however, it is practical to use symmetric coupling to avoid undesired modes with the wrong symmetry. Furthermore, we want the defect mode to couple well to the accelerating mode; part of that requirement means that the group velocity in line defect cannot be too small (on the other hand, it cannot be too large without reducing k_z). By simulating line defects over a wide range of parameters, we have identified some promising modes for coupling. Figure 6 shows the band diagram (vs. k_x, the wave number in the radial direction) for the line-channel defect. Where band 37 crosses the dotted line there is a mode with non-zero radial group velocity that is relatively isolated from other possible modes; the biggest danger comes from a mode with much higher radial phase velocity, but this mode can be avoided by proper use of symmetry.

5. Computational EM with anisotropic dielectrics

Developing new algorithms to deal with electromagnetics in dielectrics has been important to allow us to simulate dielectric accelerator structures. In the past, we demonstrated the first systematic approach to attain second order error for an embedded dielectric boundary in a finite difference algorithm [7]. Due to stability considerations, this approach works only in the frequency domain; however, from what we learned from this accurate approach, we were able to develop a more accurate (and stable) time-domain method with reduced error compared to previous algorithms [8]. This work not only presents a more accurate algorithm that corrects the failings (instability at high dielectric contrast) of earlier time-domain algorithms, but it also analyzes the accuracy of these algorithms to answer the question of whether the error is first or second order in the cell size. We found that the algorithm error could be characterized in two parts: error from the simulation of bulk dielectric, and error from simulation of the dielectric interface. The former is second order, and the latter first order; however, the latter depends on the dielectric contrast, and for low contrast does not appear until extremely high resolutions. By analyzing the error at higher contrast, we were able to show that these algorithms ultimately have first order error.

6. EM algorithms with curved metal boundaries: accuracy study

The Dey-Mittra algorithm can simulate embedded metal boundaries; a drawback of the original algorithm is the need to neglect small cell-faces and reduce the time step. We had previously shown how to choose the faces to neglect for a given time step reduction [9]. However, the effect of neglecting small cell-faces had not been previously studied. While neglecting small faces seemed to have little effect on global quantities, such as cavity eigenfrequency, it turns out they can have significant effect on the local surface fields (Fig. 7). In fact, the local surface fields cease to converge when some faces are neglected; that is, for arbitrary high resolution the error in surface fields remains the same. While that error may be sufficiently low (less than a few percent) for some applications, it is important to know that it exists. Working in the frequency domain (Fig. 7, the line with the least error), the need to neglect small faces disappears--with the appropriately reformulated matrix equation--and we demonstrated excellent scaling of a Trilinos-based eigensolver to large, parallel problems.

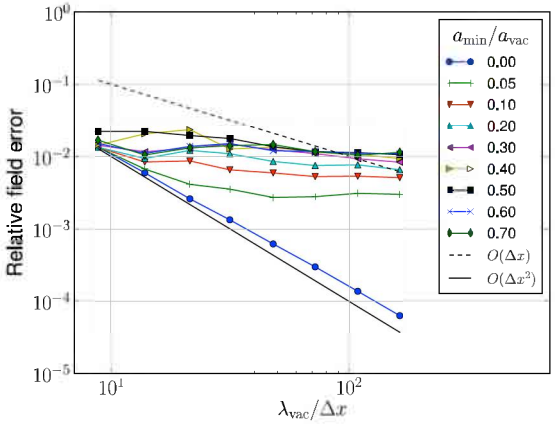

Fig. 7 Error in surface fields near a curved metal boundary.

7. Implicit EM algorithms

An implicit EM algorithm would allow arbitrarily large time step without instability; such an algorithm would be beneficial for simulating geometries with features much smaller than a wavelength--or for

simulating metal boundaries without high accuracy by avoiding the need to "drop" small cell faces. Unfortunately, implicit algorithms involve a matrix solve (inversion), which usually poses problems for scalability to large problems on parallel computers. The Alternating Direction Implicit (ADI) method seemed a promising way to obtain good performance. However, our results were mixed. While we were able to produce a reasonable parallel implementation, and achieved some improvement by optimizing the communication scheme, we felt that more work still needed to be done. In addition, while exploring the method, we found previous work [10] that pointed out a serious problem with the algorithm's accuracy, which would be it unusable for most applications. In addition, we investigated the dispersion of the algorithm and found that it also presents some possible problems that tend to go unnoticed in the literature: namely, the existence of short-wavelength modes with unphysically low frequencies. While nobody expects modes with short wavelengths (e.g., 2 cells per wavelength) to be simulated very accurately, it is a problem if the inaccuracy is so great as to reduce the frequency by orders of magnitude (down to the level of the lowest frequencies in the system). In three dimensions, we showed that the ADI dispersion (previously found in [11]) is particularly problematic in this regard. We have concluded that a better approach to implicit EM is the Crank-Nicolson approach, with a reformulated curl-curl matrix to allow efficient application of multigrid matrix-solve methods, which are known to be scalable.

8. Recent Publications

- C. A. Bauer, G. R. Werner, and J. R. Cary, "A fast multigrid-based electromagnetic eigensolver for curved metal boundaries on the Yee mesh," J. Comput. Phys. 251, 524 (2013).
- G. R. Werner, Carl A. Bauer, and John R. Cary, "A more accurate, stable, FDTD algorithm for electromagnetics in anisotropic dielectrics," J. Comput. Phys. 255, 436 (2013).
- C. A. Bauer, G. R. Werner, and J. R. Cary, "Origin and reduction of wakefields in photonic crystal accelerator cavities," PRSTAB 17, 051301 (2014).

Appendix A: Bibliography and References Cited

1 C. A. Bauer, G. R. Werner, and J. R. Cary, "Optimization of a photonic crystal cavity," J. Appl. Phys. 4 (105), 053107 (2008); DOI:10.1063/1.2973669.

2 G. R Werner, C. A. Bauer, and J. R. Cary, "Wakefields in Photonic Crystal Cavities," Phys. Rev. ST/AB **12**, 071301 (2009).

3 C. A. Bauer, "A computational study of dielectric photonic-crystal-based accelerator cavities," Ph.D. dissertation, University of Colorado, 2012.

4 C. A. Bauer, G. R. Werner, and J. R. Cary, "Origin and reduction of wakefields in photonic crystal accelerator cavities," PRSTAB 17, 051301 (2014).

5 X. E. Lin, "Photonic band gap fiber accelerator," Phys. Rev. ST Accel. Beams 4, 051301 (2001).

6 B. M. Cowan, "Three-dimensional dielectric photonic crystal structures for laser-driven acceleration," Phys. Rev. ST Accel. Beams 11, 011301 (2008).

7 C.A. Bauer, G.R. Werner, and J.R. Cary, "A second-order 3D electromagnetic algorithm for curved interfaces between anisotropic dielectrics on a Yee mesh," J. Comput. Phys. 230, 2060 (2011).

8 G. R. Werner, Carl A. Bauer, and John R. Cary, "A more accurate, stable, FDTD algorithm for electromagnetics in anisotropic dielectrics," J. Comput. Phys. 255, 436 (2013).

9 C. Nieter, J. R. Cary, G. R. Werner, D. N. Smithe, and P. H. Stoltz, "Application of Dey-Mittra conformal boundary algorithm to 3D electromagnetic modeling," J. Comput. Phys. 228, 7902 (2009).

10 S. G. Garcia and T.-W. Lee, "On the Accuracy of the ADI-FDTD Method," IEEE Antennas and Wireless Propagation Lett. 1, 31 (2002).

11 M. Darms, R. Schuhmann, H. Spachmann, and T. Weiland, "Dispersion and Asymmetry Effects of ADI-FDTD," IEEE Microwave and wireless components Lett. 12, 491 (2002).